FTIR Study of the Monosialoganglioside GM_1 in Perdeuterated Dimyristoylglycerophosphocholine ($DMPC_{d54}$) Multilamellar Bilayers: Spectroscopic Evidence of a Significant Interaction between Ca^{2+} Ions and the Sialic Acid Moiety of GM_1[†]

Maroun Bou Khalil, Morris Kates, and Danielle Carrier*

Department of Biochemistry, Microbiology, and Immunology, Faculty of Medicine, University of Ottawa, Ottawa, Ontario, Canada, K1H 8M5

Received October 5, 1999; Revised Manuscript Received January 6, 2000

ABSTRACT: Fourier transform infrared (FTIR) spectroscopy was employed to study bovine brain GM_1 and perdeuterated dimyristoylglycerophosphocholine ($DMPC_{d54}$) multilamellar dispersions (mole fractions of GM_1 in $DMPC_{d54}$: 0.12, 0.15, 0.19, 0.26, 0.34, 0.41, and 0.58), in the absence and presence of 10 mM $CaCl_2$. GM_1 micelles did not display a thermal phase transition in the temperature range 5−60 °C. Moreover, the ceramide moiety of GM_1 inserted into the hydrophobic core of $DMPC_{d54}$ bilayers and was capable of undergoing a single, cooperative phase transition (T_m = 22−28 °C, depending on GM_1 content) in a bilayer system. This suggested that the mixed bilayers consisted of a homogeneous mixture and that GM_1 was uniformly dispersed in the bilayer plane rather than segregated into regions of relative enrichment. The coexistence of GM_1 and $DMPC_{d54}$ in a bilayer environment induced a rearrangement of the interfacial hydrogen bonding network of the amide I and ester C═O groups, relative to GM_1 micelles and $DMPC_{d54}$ bilayers, respectively. The modifications induced by GM_1 might ultimately modulate surface events such as lipid−lipid and/or lipid−protein interactions. The spectroscopic results also suggested that the glycolipid's headgroup surface location and conformation in bilayers allow GM_1 to act as a receptor for Ca^{2+} via its sialic acid moiety.

Gangliosides were first discovered by Klenk in 1930 (*1*). They were recognized as the major storage lipids in the brain of children with Tay-Sachs disease (*2*). Gangliosides (Figure 1) are a large family of acidic glycosphingolipids with a common neutral tetrasaccharide to which are bound sialic acid residues, providing a corresponding number of carboxylic acid groups (*1, 3*). Brain tissue contains the highest concentrations (10 mol % of total lipids), with gangliosides GM_1[1] and GD_{1a} as the major species (*3, 4*). They are located in the extracellular leaflet of the bilayer, and their concentration there is ca. 20 mol % (*5*). Gangliosides are believed to be involved in cell−cell/substratum interactions (*6*), modulation of transmembrane signaling (*7*−*9*), alteration of membrane fluidity (*10, 11*), calcium homeostasis, and synaptic transmission (*12, 13*). Many studies ascertained the capability

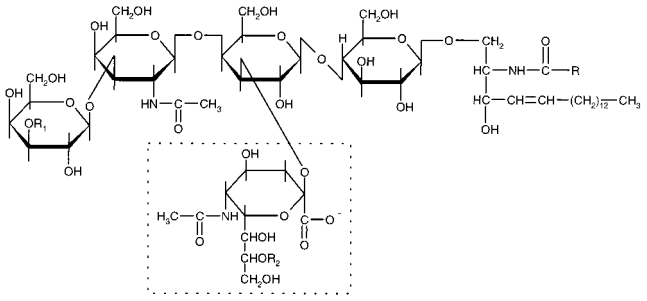

Ganglioside	R_1	R_2
GM_1	H	H
GD_{1a}	NeuNAc	H
GD_{1b}	H	NeuNAc
GT_{1b}	NeuNAc	NeuNAc

FIGURE 1: Chemical structures of the four major gangliosides (GM_1, GD_{1a}, GD_{1b}, and GT_{1b}) of mammalian brain, with the nomenclature of Svennerholm (1963). The gangliosides have a ceramide backbone and a common neutral tetrasaccharide portion (galactosyl β1→3 *N*-acetylgalactosaminyl β1→4 galactosyl β1→4 glucosyl) to which are bound sialic acid residues (structure in the dashed box with R_2 = H). NeuNAc, sialic acid; R, alkyl group.

of gangliosides to affect membrane protein activity (*14*−*17*). Cation fluxes through Na^+ and Ca^{2+} plasma membrane channels appear to be modulated by gangliosides, particularly GM_1 (*18, 19*). Garcia and Miller (*14*) and Krifuks et al. (*15*)

[†] This work was supported by a grant from the Natural Sciences and Engineering Research Council of Canada to D.C.

* To whom correspondence should be addressed at 451 Smyth Rd., Ottawa, Ontario, Canada, K1H 8M5. TEL: (613) 562-5800, ext 8215. FAX: (613) 562-5440. E-Mail: carrier@uottawa.ca.

[1] Abbreviations: AIDS, acquired immunodeficiency syndrome; CD_4, T-lymphocyte surface protein; DMPC, *sn*-1,2-dimyristoylglycero-3-phosphocholine; $DMPC_{d54}$, DMPC with perdeuterated acyl chains; DMPG, *sn*-1,2-dimyristoylglycero-3-phosphoglycerol; DPPC, *sn*-1,2-dipalmitoylglycero-3-phosphocholine; FAB MS, fast atom bombardment mass spectrometry; FTIR, Fourier transform infrared spectroscopy; GD_{xy}, disialogangliosides; GM_x, monosialogangliosides; GT_{xy}, trisialogangliosides; HIV, human immunodeficiency virus; NeuNAc, *N*-acetylneuraminic acid or sialic acid; PC, phosphatidylcholine; T_m, phase transition temperature; TLC, thin layer chromatography; x_g, mole fraction.

10.1021/bi9923104 CCC: $19.00
Published on Web 02/26/2000

showed that GM_1 preferentially elicited the down-modulation of CD_4, the binding site of HIV (the aetiologic agent of AIDS), on the surface of T-lymphocytes (*14, 15*). Gangliosides are also implicated in receptor function; e.g., GM_1 acts as the receptor of the cholera toxin (*20, 21*) and is essential to the penetration of the toxin into the cell membrane (*21*).

Single crystal X-ray structure analysis revealed that the ceramide portion of gangliosides adopts a rigid conformation, with the two hydrocarbon chains packed closely together and oriented parallelly (*10, 22, 23*). In GM_1, the region of the tetrasaccharide and the sialic acid defines an oxygen-rich surface suitable for interaction with water and cations (*24*). Abrahamsson and colleagues (1977) suggested that gangliosides tend to adopt a shovel conformation (*25*). However, data from the laboratories of many research groups suggested that gangliosides assume a linear conformation (*26, 27*).

Gangliosides in aqueous media exist in a micellar form above a critical micelle concentration of ca. 0.02 g/100 mL (*28*). Contrasted to this are the normal membrane lipids such as phosphatidylcholine (PC) which spontaneously form a lamellar structure in aqueous dispersions (*2*). Very little is known regarding the normal biological functions of gangliosides and their physical properties, partly because they are costly and difficult to synthesize. Therefore, a simple purification method was required before undertaking the investigation of the conformational and dynamic properties of these glycolipids. A modified procedure based on previously published methods was adopted for the present study (*29*−*32*). Infrared spectroscopy was used to examine the thermotropic profile of $DMPC_{d54}/GM_1$ bilayer systems (mole fractions of GM_1 in $DMPC_{d54}$: 0.12, 0.15, 0.19, 0.26, 0.34, 0.41, and 0.58). The concentration of GM_1 in the mixed $DMPC_{d54}/GM_1$ bilayers was increased to mimic physiological conditions associated with the accumulation of gangliosides in neurological disorders such as Tay-Sachs disease. Since gangliosides are involved in the regulation of Ca^{2+} homeostasis and synaptic transmission, we were also interested in determining whether this divalent cation interacts with the negatively charged sialic acid moiety of GM_1 (*3, 4*) and whether this interaction affects the hydrogen bonding of the interfacial region, the dynamics of the lipid hydrocarbon chains, and the phase behavior of the mixed $DMPC_{d54}/GM_1$ bilayers. We report the results of such studies using FTIR spectroscopy.

MATERIALS AND METHODS

Reagents. All chemicals used were of analytical quality and obtained from VWR Scientific of Canada Ltd.: MWCO 500 Spectra/Pro Cellulose Ester dialysis membrane (20 mm diameter), Diamond K6F silica gel precoated thin-layer plates (60 Å, 2.5 × 7.5 cm, and 5.0 × 10 cm, 250 μm layer thickness), and silica gel (Kieselgel G, 230−400 mesh). DEAE-Sepharose CL-6B (mean particle size 90 μm, particle size range 45−165 μm in wet form) was obtained from Pharmacia. Synthetic perdeuterated $DMPC_{d54}$ was purchased from Avanti Polar Lipids and used without further purification for FTIR analysis. Gangliosides GM_1 and GT_{1b}, bought from Sigma Chemical Co., were used as standards for thin layer chromatography (TLC) analysis. Deuterated water was from MSD Isotopes (Montréal, Québec, Canada). Bovine brains were obtained from a local slaughterhouse (Ottawa, ON, Canada).

Isolation and Purification of Bovine Brain GM_1. The original method of Folch et al. (1957) (*29*), as modified by Svennerholm and Fredman (1980) (*30*), was used for the extraction of total lipids and the purification of gangliosides. Bovine brain tissue lipids and gangliosides were extracted with 20 volumes of $CHCl_3/CH_3OH$/water (4:8:3, v/v/v). The solvent composition was adjusted to 4:8:5.6 (v/v/v) for ganglioside partitioning. The lower chloroform phase was repartitioned by addition of 0.5 volume of methanol and 0.33 volume of 0.01 M potassium chloride. The crude gangliosides isolated from the upper water-enriched phase were freed from low molecular weight contaminants by dialysis against deionized water. The crude preparation contained sulfatides and various phospholipid contaminants. Bovine brain gangliosides were separated from the much larger quantity of neutral, zwitterionic, and acidic lipids (e.g., cholesterol, lecithin, ethanolamine phosphoglycerides, cerebrosides, neutral glycolipids, free fatty acids, sulfatides, serine, and inositol phosphoglycerides) by anion exchange chromatography as described by Fredman et al. (1980) (*31*) with the following modifications: DEAE-Sepharose (200 mL) was used for its high binding capacity and good separation, and monosialogangliosides were eluted with potassium acetate in methanol (0.02 M), instead of ammonium acetate, because the latter produces an acidic solution upon its removal by evaporation and induces a spontaneous hydrolysis of the sialic acid moiety in the oligosaccharide chain (*31, 32*). A subsequent, final step of silicic acid column chromatography (100 g) is then required to remove the contaminating acidic lipids and to ensure also the removal of small amounts of protein that may have survived the preceding treatment (*31*). Gangliosides were detected by TLC in $CHCl_3/CH_3OH$/0.20% $CaCl_2$ (60:40:9, v/v/v) (*3*) and stained with resorcinol (*3, 33*) and α-naphthol (*34*).

Preparation of Micellar Solutions and Multilamellar Bilayers. Suspensions of pure bovine brain GM_1 and dispersions of $DMPC_{d54}$ and $DMPC_{d54}/GM_1$ (mole fractions of GM_1 in $DMPC_{d54}$: 0.12, 0.15, 0.19, 0.26, 0.34, 0.41, and 0.58) were prepared as follows: the lipids, dissolved in $CHCl_3/CH_3OH$ (2:1, v/v), were dried under a stream of nitrogen and left overnight under vacuum. Multilamellar dispersions (10% w/v) were prepared by vortex-mixing the dry lipids with the appropriate amounts of ^2H_2O (p^{2}H 7.5) or H_2O (pH 7.5) without Ca^{2+} or with 10 mM $CaCl_2$. At least four freeze (liquid nitrogen, −80 °C)/thaw (water bath, 80 °C) cycles were performed to ensure a homogeneous organization of the liposomes. GM_1 micelles (10% w/v) and $DMPC_{d54}$ bilayers (10% w/v) were prepared in the same manner.

FTIR Spectroscopic Analysis. Samples for thermotropic studies were placed between two calcium fluoride windows separated by a 6 μm spacer. FTIR spectra were recorded on a Digilab FTS-40A spectrometer equipped with a liquid nitrogen cooled mercury−cadmium−telluride detector (MCT); measurements were made over 2−5 °C intervals in the range 5−60 °C, using a thermostated cell mount and variable-temperature water bath. For each spectrum, 256 interferograms were accumulated with a spectral resolution of 2 cm^{-1}. The instrument was purged continuously with dry air to eliminate spectral contributions from atmospheric water vapor. Fourier self-deconvolution of overlapping amide I (1590−1660 cm^{-1}) and ester C═O (1700−1760 cm^{-1}) bands was performed using the resolution enhancement procedure

of Kauppinen et al. (1981) (*35*) with a bandwidth of 17 and a breakpoint of 1.5. Frequencies of the methylene symmetric C−H (2850−2855 cm^{-1}) and C−D (2089−2099 cm^{-1}), phosphate asymmetric (1160−1300 cm^{-1}), amide I, and ester C═O stretching vibrations were determined with the aid of the third-order Fourier derivative (*36*) with a power of 3 and a breakpoint of 0.3. The T_m values of the mixed $DMPC_{d54}/GM_1$ bilayers were estimated from the first-derivative plots of the methylene symmetric C−H (C−D) stretching vibration frequency vs temperature.

RESULTS

Characterization of GM_1. Thin-layer chromatography of the crude ganglioside extract in the solvent system $CHCl_3/CH_3OH/0.20\%$ $CaCl_2$ (60:40:9, v/v) (*3*) and staining with resorcinol (*3*, *43*) and α-naphthol (*44*) revealed the presence of GM_3, GM_2, GM_1, GD_{1a}, GD_{1b}, and GT_{1b}; the monosialoganglioside GM_1 and the disialogangliosides GD_{1a} and GD_{1b} being the major species (results not shown). The final purity of GM_1, isolated by the procedure of Folch et al. (1957) (*39*), as modified by Svennerholm and Fredman (1980) (*40*), was greater than 99% as judged by TLC [R_f 0.49 reported value for human white and gray matter (*3*)]. Negative FAB mass spectra of underivatized bovine brain GM_1 (results not shown) revealed a major ion peak at *m*/*z* 1544 corresponding to the molecular ion $(M-H)^{-1}$, based on stearic acid (18:0) as the major acyl group. Ion peaks due to several fragments formed by cleavage at the glycosidic linkages from the nonreducing terminal were detected at *m*/*z* 1382, formed by cleavage of the galactose residue from GM_1; *m*/*z* 1179, formed after cleavage of the *N*-acetylgalactosamine residue from the *m*/*z* 1382 fragment; *m*/*z* 888, formed after the sialic acid moiety was cleaved from the *m*/*z* 1179 fragment; and at *m*/*z* 282, corresponding to the major stearic acid moiety of GM_1. In addition, fragment ions pertaining to the minor fatty acids of GM_1 (16:0 > 15:0 > 18:2 ≥ 20:4 > 20:0 ≥ 16:1 > 14:1 > 14:0) were also detected. The long-chain base consisted mainly of sphingosine 18:1 as indicated by the ion peak at *m*/*z* 281. The results reported here on the composition and heterogeneity of the fatty acyl groups of bovine brain GM_1 are in agreement with those reported in the literature (*3*, *37*−*39*).

The Interfacial Region of $DMPC_{d54}/GM_1$ Bilayers (Amide I and Ester C═O Groups). Amide groups of gangliosides (Figure 1) give rise to characteristic vibrational bands in their infrared spectra. The amide I band (1590−1660 cm^{-1}) originates from the C−O stretching vibration with a small contribution of the C−N stretching and N−H bending vibrations, while the amide II band (1500−1580 cm^{-1}) arises principally from the N−H bending and C−N stretching vibrations (*40*). The infrared spectra of GM_1 show complex patterns in the amide I absorption region due to the presence of three amide groups and a carboxylate group in the molecule. The deprotonated form of the carboxylate group of the sialic acid moiety absorbs in the frequency region of the amide I vibrational band (*41*). To simplify the spectrum, ^2H_2O was used as a solvent for this study, since H/D exchange at the amide groups induces a shift of the amide II band to wavenumbers lower than 1500 cm^{-1} (*41*). In addition, the deformation mode of deuterated water is observed at ca. 1250 cm^{-1} instead of 1640 cm^{-1}. With ^2H_2O as a solvent, the amide I and ester carbonyl stretching bands

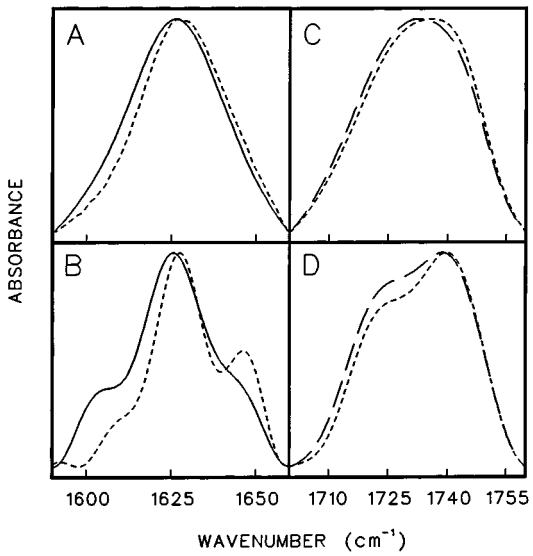

FIGURE 2: Amide I C═O stretching region of the infrared spectrum of a GM_1 micellar solution (solid line) and a $DMPC_{d54}/GM_1$ dispersion (small dashes), before (A) and after (B) deconvolution. Ester C═O stretching region of the infrared spectrum of a dispersion of $DMPC_{d54}$ (long dashes) and $DMPC_{d54}/GM_1$ (small dashes), before (C) and after (D) deconvolution. The spectra were autoscaled. The samples were prepared in ^2H_2O (p^2H 7.5), and the $DMPC_{d54}/GM_1$ dispersion had a GM_1 mole fraction of 0.26.

are thus the only vibrational modes left in the frequency range 1500−1800 cm^{-1}, together with the C═C stretching bands due to the chains unsaturations.

The amide I (1590−1660 cm^{-1}) and the ester carbonyl (1700−1760 cm^{-1}) stretching modes of GM_1 and $DMPC_{d54}$, respectively, were examined to assess the degree of hydrogen bonding at the interfacial region (*42*, *43*). In the mixed $DMPC_{d54}/GM_1$ bilayers, the amide I C═O band arising from GM_1 (Figure 2, panel A, small dashes) is found at 1630 cm^{-1}, as compared to 1625 cm^{-1} for the GM_1 micellar suspensions (Figure 2, panel A, solid line). Upon deconvolution of the original spectra, the amide I absorption band of GM_1 micelles (Figure 2, panel B, solid line) is found to be the sum of three overlapping bands centered at 1640, 1625, and 1605 cm^{-1}. In the mixed $DMPC_{d54}/GM_1$ bilayer systems (panel B, small dashes), these three amide I constituent bands shifted to higher frequencies: 1645, 1630, and 1610 cm^{-1}. Therefore, the amide I component bands at 1625 cm^{-1}, for GM_1 micelles, and at 1630 cm^{-1}, for $DMPC_{d54}/GM_1$ bilayers, were assigned to the amide groups that are involved in hydrogen bonding, and the high-frequency constituent bands at 1640 cm^{-1}, for GM_1 micelles, and at 1645 cm^{-1}, for $DMPC_{d54}/GM_1$ bilayers, were assigned to the ones that are less involved in hydrogen bonding at the interfacial region (*44*). Müller and Blume (1993) have shown that the third component band has too low a frequency to pertain to an amide I band, and they have assigned it to the CO_2^- group of the sialic acid moiety of GM_1 (*41*).

Similarly, the ester C═O band arising from $DMPC_{d54}$ in the mixed bilayers (Figure 2, panel C, small dashes) shifted to a higher frequency, 1740 cm^{-1}, as compared to 1732 cm^{-1} for the $DMPC_{d54}$ dispersions (Figure 2, panel C, long dashes). In the infrared spectral region 1700−1760 cm^{-1}, the Fourier deconvolved spectra of $DMPC_{d54}$ (Figure 2, panel D, long dashes) and of mixed $DMPC_{d54}/GM_1$ bilayers (Figure 2, panel D, small dashes) revealed overlapping bands at 1725 and

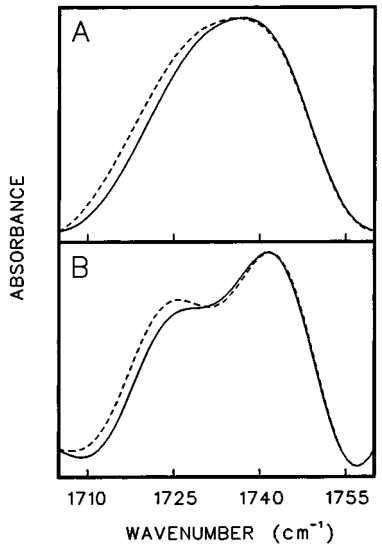

FIGURE 3: Ester C═O stretching region of the infrared spectrum of a $DMPC_{d54}/GM_1$ dispersion with a GM_1 mole fraction of 0.26 without Ca^{2+} (solid line) or with 10 mM $CaCl_2$ (small dashes) before (A) and after (B) deconvolution. The spectra were autoscaled. The samples were prepared in ^2H_2O (p^2H 7.5).

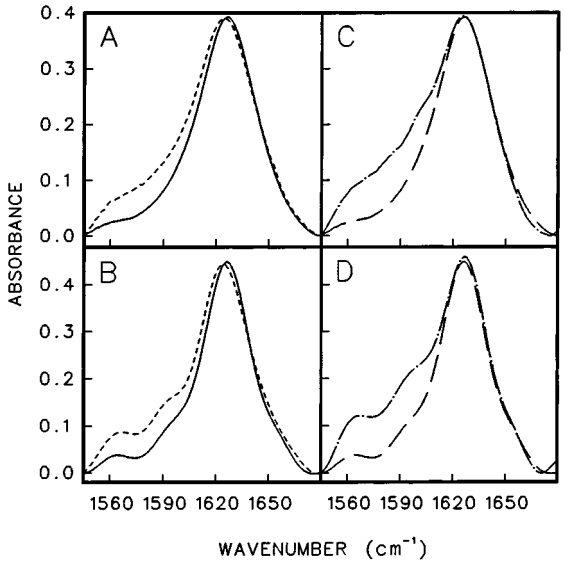

FIGURE 4: Carboxylate asymmetric and amide I C═O stretching region of the infrared spectra of a GM_1 micellar suspension without Ca^{2+} (solid line) or with 10 mM $CaCl_2$ (small dashes), before (A) and after (B) deconvolution, and of a $DMPC_{d54}/GM_1$ dispersion with a GM_1 mole fraction of 0.26 without Ca^{2+} (long dashes) or with the cation (dot−long dash), before (C) and after (D) deconvolution. The spectra were normalized with the integrated intensity of the methylene symmetric C−H stretching band. All the samples were prepared in ^2H_2O (p^2H 7.5) without or with 10 mM $CaCl_2$, as indicated.

1745 cm^{-1}, assigned to ester C═O groups involved and less involved in hydrogen bonding, respectively (*44*, *45*). A decrease in the relative intensity of the 1725 cm^{-1} component band (panel D, small dashes) was observed in the mixed bilayers, indicative of a reduction in the population of hydrogen bonded ester C═O groups of $DMPC_{d54}$. The observed shift to higher frequencies for the amide I and ester C═O vibrational modes indicates that the C═O groups at the interfacial zone of the mixed $DMPC_{d54}/GM_1$ bilayers display an increased double bond character and reduced hydrogen bonding (*44*, *45*).

The effect of Ca^{2+} ions on the interfacial hydrogen bonding and the hydrocarbon chain dynamics of the mixed $DMPC_{d54}/GM_1$ bilayers was also assessed by FTIR. The addition of Ca^{2+} ions to a $DMPC_{d54}/GM_1$ dispersion with a GM_1 mole fraction of 0.26 led to a frequency shift of the ester C═O absorption band from 1740 to 1730 cm^{-1} (Figure 3, panel A). In the absence of Ca^{2+} and upon Fourier deconvolution (Figure 3, panel B, solid line), the $DMPC_{d54}/GM_1$ spectra revealed high- and low-frequency constituent bands centered at 1740 and 1725 cm^{-1}, respectively. In the presence of Ca^{2+} ions, the ester C═O component band at 1725 cm^{-1} was observed at 1722 cm^{-1} and increased in its relative intensity (Figure 3, panel B, small dashes). The shift of the ester C═O band to lower frequency suggests a strengthened hydrogen bonding network (*44*, *45*) at the bilayer interfacial zone of the mixed $DMPC_{d54}/GM_1$ bilayers that could be due to a tightening of the lipidic network following neutralization by Ca^{2+} ions.

Interaction of Ca^{2+} with the Carboxylate Moiety of GM_1 and the Phosphate Moiety of $DMPC_{d54}$ in the Mixed Bilayers. The negatively charged gangliosides have the potential to bind cations on the cell surface, and this binding may be of importance in cell physiology. Ca^{2+} can bind to the sialic acid residue of GM_1 as well as to the phosphate group of $DMPC_{d54}$. Hayashi et al. (1984) observed that brain gangliosides in the micellar form were able to bind more Ca^{2+} ions (ca. 0.6 Ca^{2+} per ganglioside molecule) than the tested isolated phospholipid species (PS and PI) (*46*). In the absence of Ca^{2+}, the region 1500−1800 cm^{-1} of the infrared spectra of GM_1 micellar suspensions (Figure 4, panel A, solid line) and $DMPC_{d54}/GM_1$ dispersions with a GM_1 mole fraction of 0.26 (Figure 4, panel C, long dashes) reveal two major absorption bands: the amide I vibration band of GM_1 at 1625 cm^{-1} and the carboxylate asymmetric stretching vibration band at 1560 cm^{-1}. In the presence of the divalent cation (Figure 4, panel A, small dashes), the amide I band of GM_1 micelles shifted to 1620 cm^{-1}, and the carboxylate band remained at ca. 1560 cm^{-1} but changed significantly in its band shape and intensity. Deconvolution of the original spectra showed that each of these absorption bands is the sum of several overlapping bands (Figure 4, panels B and D). In the absence of Ca^{2+} ions, two component bands are observed at ca. 1560 and 1590 cm^{-1} for the asymmetric carboxylate stretching band of GM_1 micelles (Figure 4, panel B, solid line) and in the mixed $DMPC_{d54}/GM_1$ bilayers (Figure 4, panel D, long dashes). In the presence of 10 mM $CaCl_2$, the two peaks changed in their relative intensity and band shape for GM_1 micelles (Figure 4, panel B, small dashes) and $DMPC_{d54}/GM_1$ bilayers (Figure 4, panel D, dot−long dash). On the other hand, the frequency of the asymmetric phosphate vibrational band of the phospholipid has shifted from 1230 cm^{-1} (Figure 5, panel A, solid line) to 1231 cm^{-1} (Figure 5, panel A, small dashes) for $DMPC_{d54}$ dispersions and remained at ca. 1230 cm^{-1} for $DMPC_{d54}/GM_1$ bilayers (Figure 5, panel B) in the presence of the divalent cation. These Ca^{2+}-induced changes of the phosphate band of $DMPC_{d54}$ (Figure 5) are not as significant as the previously reported ones for dimyristoylglycerophosphoglycerol (DMPG): the asymmetric phosphate stretching band of DMPG shifted to lower frequencies by 2−8 cm^{-1} in the presence of cationic molecules (*47*, *48*).

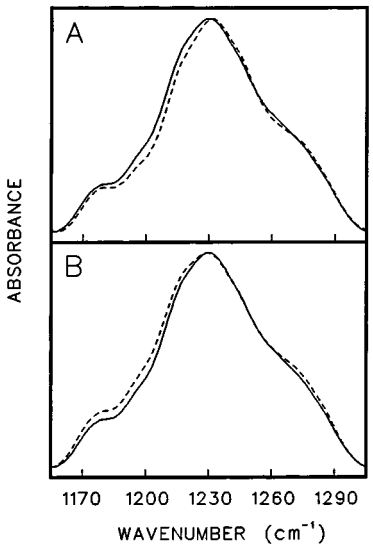

FIGURE 5: Phosphate asymmetric stretching region of the infrared spectrum of $DMPC_{d54}$ (panel A) and a $DMPC_{d54}/GM_1$ dispersion with a GM_1 mole fraction of 0.26 (panel B) in H_2O (pH 7.5) without Ca^{2+} (solid line) or with 10 mM $CaCl_2$ (small dashes). The spectra were autoscaled.

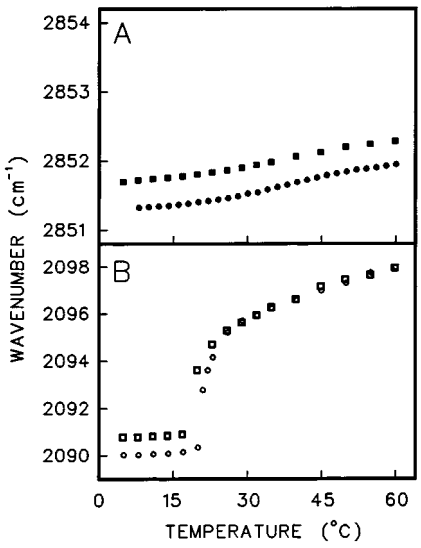

FIGURE 6: Temperature dependence of the symmetric C−H (panel A) and C−D (panel B) stretching vibrations of the methylene groups of GM_1 and $DMPC_{d54}$, respectively, before (■ and □) and after (● and ○) the addition of Ca^{2+}. (A) Temperature profile of GM_1 micellar suspensions in ^2H_2O (p^2H 7.5) without Ca^{2+} (■, $n = 4$) or with 10 mM $CaCl_2$ (●, $n = 4$). (B) Temperature profile of $DMPC_{d54}$ dispersions in ^2H_2O (p^2H 7.5) without Ca^{2+} (□, $n = 4$) or with 10 mM $CaCl_2$ (○, $n = 4$).

The infrared data reported in this study indicate that Ca^{2+} ions interact with the negatively charged carboxylate group of the sialic acid residue of GM_1 to a much greater extent than with the phosphate moiety of $DMPC_{d54}$. Therefore, the fact that, upon Ca^{2+} binding, the asymmetric carboxylate vibrational band of GM_1 underwent dramatic changes in contrast to the slight spectral changes in the phosphate absorption band of $DMPC_{d54}$ indicates that the divalent cation preferentially binds to the glycolipid even in the mixed $DMPC_{d54}/GM_1$ bilayers, neutralizing the negative charge of its carboxyl group and possibly cross-linking two GM_1 molecules in the bilayer plane.

Thermotropic Phase Behavior of Pure GM_1 and $DMPC_{d54}$. The temperature dependence of the frequency of the methylene symmetric C−H (ca. 2850 cm^{-1}) and C−D (ca. 2090 cm^{-1}) stretching bands allows us to monitor the dynamics of the lipidic chains. The maxima of these absorption bands are typically shifted by about 2−3 cm^{-1} to higher wavenumbers at the lamellar gel to liquid-crystalline phase transition due to an increase of disorder or mobility of the acyl chains (*41*). The thermotropic profile of GM_1 micellar suspensions [110 mg/mL, well beyond the critical micelle concentration (0.02 g/mL)] exhibits no sign of a cooperative phase transition in the temperature range of 5−60 °C without Ca^{2+} (Figure 6, panel A, ■) or with 10 mM $CaCl_2$ (Figure 6, panel A, ●). There is a gradual increase in the frequency of the methylene symmetric C−H stretching vibration upon increasing temperature, with no discontinuity that could indicate a phase transition. This smooth thermotropic profile suggests that GM_1 was still in the micellar form, which is in agreement with the absence of transition in pure unsonicated suspensions of GM_1 (4 mg/mL) reported by Sillerud et al. (1979) (*49*) and in pure sonicated suspensions of GM_1 and GD_{1a} (15 mg/mL) reported by Hinz et al. (1981) (*50*). In contrast, the frequency of the acyl chains of $DMPC_{d54}$ increased gradually upon raising the temperature from 5 to 60 °C, with a well-defined and cooperative phase transition centered at 19 °C (Figure 6, panel B, □) in the absence of Ca^{2+} ions, and at 21 °C (Figure 6, panel B, ○) in the presence of the divalent cation. The frequencies of the methylene symmetric C−H ($\upsilon_s CH_2$) and C−D ($\upsilon_s CD_2$) stretching vibration bands of GM_1 (Figure 6, panel A, ●) and $DMPC_{d54}$ (Figure 6, panel B, ○), respectively, are lowered in the presence of Ca^{2+}, indicating that the divalent cation exerts an ordering effect on the acyl chains of GM_1 micelles and on those of $DMPC_{d54}$ bilayers in the gel phase.

Measurements on the Mixed $DMPC_{d54}/GM_1$ Bilayers. Synthetic $DMPC_{d54}$ was used as a host phospholipid. The use of perdeuterated acyl chains provides a useful means to circumvent problems associated with interferences from the CH_2 symmetric (2850 cm^{-1}) stretching vibrations by GM_1. FTIR measurements were made on the following mole fractions of GM_1 in $DMPC_{d54}$: 0.12, 0.15, 0.19, 0.26, 0.34, 0.41, and 0.58. The influence of GM_1 on the phase behavior of $DMPC_{d54}$ can be monitored by following the frequency of the CD_2 symmetric stretching vibrational band at ca. 2090 cm^{-1} as a function of temperature. The addition of GM_1 to $DMPC_{d54}$ bilayers leads to increased gel/liquid-crystalline phase transition temperatures with increasing ganglioside content (Table 1). While the thermotropic profile of pure $DMPC_{d54}/Ca^{2+}$ vesicles reveals a single, sharp transition at ca. 21 °C (Figure 7, panels B and D, ○), $DMPC_{d54}$ dispersions containing GM_1 and Ca^{2+} exhibit a single, smooth transition between ca. 22 and 28 °C, depending on the GM_1 concentration. In the mixed $DMPC_{d54}/GM_1$ bilayers, the thermotropic profiles of the hydrocarbon chains of GM_1 and of the perdeuterated acyl chains of $DMPC_{d54}$ were similar, and the gel/liquid-crystalline transition temperatures were identical (±0.3 °C) for the methylene C−H (2850 cm^{-1}) (Figure 7, panels A and C) and C−D (2090 cm^{-1}) (Figure 7, panels B and D) symmetric stretching vibrations. For GM_1 molar fractions of 0.12 (Figure 7, ■ and □), the order−disorder T_m for $DMPC_{d54}/GM_1$ dispersions was 22 °C. The gel to liquid-crystalline phase transition for the mixed bilayers was 26 °C for GM_1 molar fractions of 0.26 (Figure 7, ▼ and

Table 1: Gel to Liquid-Crystalline Transition Temperature of Dispersions of $DMPC_{d54}$ and $DMPC_{d54}/GM_1/Ca^{2+}$ [a]

$DMPC_{d54}/GM_1$ molar ratio	GM_1 mole fraction	transition temperature (±1 °C)	
		$DMPC_{d54}$	GM_1
1:0	–	21	–
0:1	–	–	no transition
1:0.07	0.12	22	22
1:0.08	0.15	23	23
1:0.11	0.19	25	25
1:0.17	0.26	26	26
1:0.25	0.34	26	26
1:0.33	0.41	28	28
1:0.66	0.58	28	28

[a] The transition temperatures (the average of 4 repeats for each experiment in the temperature range 5−60 °C) were obtained from the CD_2 ($DMPC_{d54}$) and CH_2 (GM_1) symmetric stretching vibrations in the infrared spectra. The GM_1 micellar suspensions as well as the $DMPC_{d54}$ and $DMPC_{d54}/GM_1$ dispersions were prepared in ^2H_2O (p^2H 7.5) with 10 mM $CaCl_2$.

▽) and 0.34 (Figure 7, ▲ and △). At high ganglioside concentration, the phase transition temperature of $DMPC_{d54}/GM_1$ dispersions stayed at 28 °C from a GM_1 molar fraction of 0.41 (Figure 7, +) to 0.58 (Table 1). A characteristic feature of the $DMPC_{d54}/GM_1$ mixtures (Figure 7) is the presence of a single and cooperative transition, suggesting that the two lipids were completely miscible, at all GM_1 concentrations, in both the gel and the liquid-crystalline phase. Our results are in agreement with those of Müller and colleagues (1993, 1996) (*41*, *51*).

The effect of Ca^{2+} on the phase behavior of the mixed $DMPC_{d54}/GM_1$ bilayers (GM_1 $x_g = 0.26$) is shown in Figure 8. The order−disorder T_m of the hydrocarbon chains of the glycolipid (panel A, ×) and of the perdeuterated acyl chains of the phospholipid (panel B, ×) is 23 °C in the absence of Ca^{2+}. The divalent cation induced a shift of the transition temperature to 26 °C, suggesting a reduction of the mobility and disorder of the acyl chains of GM_1 (panel A, ▼) and $DMPC_{d54}$ (panel B, ▽) and thus a stabilization of the mixed bilayers. The $\upsilon_s CH_2$ of GM_1 (Figure 8, panel A, ▼) and $\upsilon_s CD_2$ of $DMPC_{d54}$ (Figure 8, panel B, ▽) are lowered in the presence of Ca^{2+}, indicating that the mixed bilayers contained fewer gauche conformers and that the acyl chains were packed tightly in the hydrophobic core of the $DMPC_{d54}$ bilayer. Similarly, the Ca^{2+}-induced shift of the T_m to higher temperatures was also pronounced for the mixed $DMPC_{d54}/GM_1$ bilayers (GM_1 $x_g = 0.34$), where the T_m increased from 24 to 26 °C (results not shown). Therefore, the ordering effect of GM_1 on $DMPC_{d54}$ bilayers is enhanced by the presence of Ca^{2+} ions.

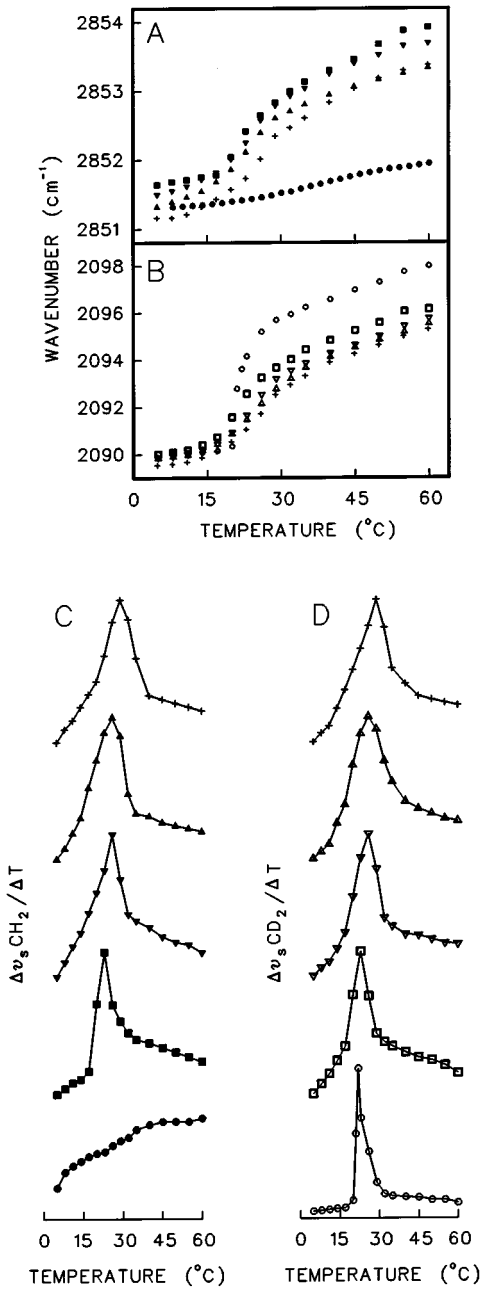

FIGURE 7: (A) Temperature dependence of the methylene symmetric C−H stretching vibration of GM_1 micellar suspensions (●) and $DMPC_{d54}/GM_1$ mixtures with GM_1 mole fractions of 0.12 (■), 0.26 (▼), 0.34 (▲), and 0.41 (+). (B) Temperature dependence of the methylene symmetric C−D stretching vibration of $DMPC_{d54}$ dispersions (○) and $DMPC_{d54}/GM_1$ mixtures with GM_1 mole fractions of 0.12 (□), 0.26 (▽), 0.34 (△), and 0.41 (+). (C) First-derivative plots of the curves shown in panel A. (D) First-derivative plots of the curves shown in panel B. All the samples were prepared in ^2H_2O (p^2H 7.5) with 10 mM $CaCl_2$.

DISCUSSION

The main purpose of the present spectroscopic investigation was to elucidate the biochemical significance of GM_1 in a $DMPC_{d54}$ bilayer environment. We were also interested in examining the effect of GM_1 on the phase behavior of $DMPC_{d54}$ and in studying the interaction of the glycolipid with Ca^{2+} ions to shed some light on its involvement in the regulation of synaptic transmission. GM_1 is an amphiphilic molecule present on the outer leaflet of the plasma membrane, and it is plausible that this glycolipid, along with other negatively charged lipids comprised in the interfacial region of the bilayer, may serve as an anionic site to trap Ca^{2+} and other cations of biological significance. The ceramide moiety of bovine brain GM_1, used throughout this study, is a mixture of fatty acid molecular species with different hydrocarbon chain lengths, stearic acid being the major species (*3*, *37*−*39*). The fluidity of the hydrophobic core of GM_1 micelles increased gradually with temperature, but no thermal phase transition was observed by FTIR spectroscopy (Figure 6). Hirai and Takizawa (1998) reported that the elevation of temperature (from 6 to 60 °C) induced a significant shrinkage of the hydrophilic region of the ganglioside micellar suspen-

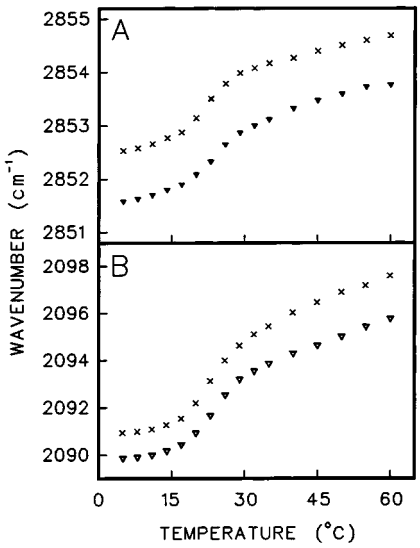

FIGURE 8: Temperature dependence of the symmetric C−H (panel A) and C−D (panel B) stretching vibrations of the methylene groups of GM_1 and $DMPC_{d54}$, respectively, before and after the addition of Ca^{2+}. (A) Temperature profile of a $DMPC_{d54}/GM_1$ dispersion with a GM_1 mole fraction of 0.26 in ^2H_2O (p^2H 7.5) without Ca^{2+} (×, $n = 4$) or with 10 mM $CaCl_2$ (▼, $n = 4$). (B) Temperature profile of a $DMPC_{d54}/GM_1$ dispersion with a GM_1 mole fraction of 0.26 in ^2H_2O (p^2H 7.5) without Ca^{2+} (×, $n = 4$) or with 10 mM $CaCl_2$ (▽, $n = 4$).

sions. The authors concluded that gangliosides can act like a water cavity, reversibly entrapping or releasing large amounts of water and thus modulating the local hydrophobicity of the cell surface (*52*). On the other hand, $DMPC_{d54}$ forms bilayers in aqueous dispersions. The gel to liquid-crystalline phase transition of $DMPC_{d54}$ was centered at 19 °C without Ca^{2+} and at 21 °C with 10 mM $CaCl_2$, suggesting that the divalent cation had an ordering effect on the hydrocarbon region of the bilayer.

The interactions that GM_1 can establish with synthetic $DMPC_{d54}$ should provide a better understanding in molecular terms of the ability of the glycolipid to induce changes in membrane permeability and stability. In the mixed $DMPC_{d54}/GM_1$ bilayer systems with varying GM_1 molar fractions, the hydrocarbon chains of GM_1 exhibited a phase transition with an order−disorder T_m identical (±0.3 °C) to that of the perdeuterated acyl chains of $DMPC_{d54}$ and occurring at a higher temperature than in pure $DMPC_{d54}$ dispersions. This indicated that GM_1 was incorporated into $DMPC_{d54}$ bilayers and was capable of undergoing a phase transition in a lipid bilayer environment. It was suggested earlier that such thermal phase transitions of glycolipids may be influenced by rearrangements of their large polar headgroups (*53*). The presence of a single, cooperative phase transition is consistent with homogeneous mixing of $DMPC_{d54}$ and GM_1 within the mixed bilayers, without lateral phase segregation. The addition of GM_1 to $DMPC_{d54}$ bilayers increased the transition temperature of the phospholipid, with the acyl chains becoming motionally restricted relative to $DMPC_{d54}$. Ca^{2+} ions further enhanced the ordering effect of the glycolipid on the hydrocarbon chains of $DMPC_{d54}$.

Since the ceramide moiety of GM_1 comprises fatty acyl chains longer than the perdeuterated myristoyl chain of $DMPC_{d54}$, its insertion into the bilayer hydrophobic core affects the packing of the perdeuterated hydrocarbon chains. Dahlen and Pascher (1979) have suggested that the sphingosine chain of glycosphingolipids penetrates into the bilayer by only 14 carbons (*54*). Boggs and Koshy (1994) have suggested that the carbohydrate headgroup of cerebroside sulfate (CBS) protrudes above the surface of PC bilayers, allowing the sulfoglycolipid to be recognized by various carbohydrate binding ligands and proteins (*55*). Both GM_1 ganglioside and $DMPC_{d54}$ can probably bind or at least interact with divalent cations such as Ca^{2+}. Whether the binding affinity of Ca^{2+} toward GM_1 is greater than to $DMPC_{d54}$ was still unclear. Our results show that the divalent cation induces important changes of the GM_1 sialic acid carboxylate band in the mixed $DMPC_{d54}/GM_1$ bilayers, suggesting a direct interaction, whereas the $DMPC_{d54}$ phosphate band is not affected significantly. Based on the interpretations of Dahlen and Pascher (1979) and Boggs and Koshy (1994), we concluded that the carbohydrate headgroup of GM_1 protrudes out of the $DMPC_{d54}$ bilayer surface, allowing a better binding of Ca^{2+} ions to the glycolipid than to the phospholipid (*54, 55*).

Müller and colleagues (1993, 1996) conducted a series of FTIR studies on $DMPC/GM_1$ bilayers and concluded that the affinity of Ca^{2+} ions toward the phosphate moiety of DMPC is greater than to the sialic acid moiety of GM_1 (*41, 51*). They reported that the band shape and relative intensity of the asymmetric carboxylate stretching band of GM_1 in the infrared spectrum did not change in the mixed $DMPC/GM_1$ bilayers (5:1, mol/mol) when the divalent cation was present. The surface location and the conformation of the headgroup region of gangliosides govern their ability to interact with ions and carbohydrate binding ligands. The unique surface position of the headgroup region of GM_1 is determined by the fatty acid chains of the ceramide backbone of the glycolipid. The contradictory results presented by Müller and colleagues (1993, 1996) (*41, 51*) may be attributed to the use of different fatty acid chain lengths, to the different degree of saturation of the GM_1 acyl chains, and to the conformation of the oligosaccharide moiety, which would ultimately affect the surface location of the glycolipid and its interaction with various ligands, specifically Ca^{2+} ions.

The changes in the amide I and ester C═O absorption bands in the mixed $DMPC_{d54}/GM_1$ bilayers revealed that hydrogen bonding was disrupted in the absence of Ca^{2+} ions, as compared to GM_1 micelles and $DMPC_{d54}$ bilayers. The perfect mixing of GM_1 and $DMPC_{d54}$ impedes hydrogen bonding between the glycolipid molecules. On the other hand, GM_1 gives a tighter bilayer, decreasing the accessibility of water molecules to $DMPC_{d54}$ and GM_1 in the mixed bilayers. Therefore, the most likely interaction is then between the two types of lipids. The complex formation of Ca^{2+} with GM_1 in the mixed bilayers increased hydrogen bonding: the neutralization of the negatively charged sialic acid residues of GM_1 by interaction with Ca^{2+} affects the orientation of the sialic acid residue at the interfacial zone (*56*) of $DMPC_{d54}$ bilayers, which would ultimately influence the molecular packing of the acyl chains in the bilayer. These modifications in the headgroup region of GM_1 modify hydration at the interface, leading to increased hydrophobic chain interactions and intermolecular cohesion, which brings the oligosaccharide moiety of GM_1 and the headgroup of

$DMPC_{d54}$ closer and, thus, strengthens the hydrogen bonding network.

The following model was suggested for the implication of GM_1 in synaptic transmission and Ca^{2+} homeostasis at the presynaptic membrane. The negatively charged sialic acid residues of GM_1 bind Ca^{2+} (*12*, *46*, *57*), and the synaptic membrane is tightened or rigidified. The stabilizing effect of Ca^{2+} on the lipid bilayer is most likely attributed to intermolecular bridging effects of Ca^{2+} (*56*). When an action potential arrives at the synapse, Ca^{2+} is displaced from the gangliosides and the hydrogen bonding network is disrupted, thus increasing the fluidity of the plasma membrane and inducing increased permeability for the divalent cation. The entry of calcium to the intracellular space could be facilitated via ganglioside-modulated ion channels. The transmitter is released, and Ca^{2+} is pumped out of the neuroplasm by means of ganglioside-modulated membrane proteins. The divalent cation then rebinds to gangliosides, which induces a retightening of the membrane for a new transmission cycle (*12*−*14*).

In summary, membrane ganglioside concentration is typically low, and these molecules are most likely randomly distributed in the bilayer plane, notably because they are anionic and would be expected to repulse each other. The results reported here clearly show that GM_1 is incorporated and molecularly dispersed in the mixed $DMPC_{d54}/GM_1$ bilayers, without lateral phase separation of the lipid components. Furthermore, GM_1-bound Ca^{2+} ions and GM_1/Ca^{2+} interactions were more pronounced than those of $DMPC_{d54}/Ca^{2+}$. The evidence of ganglioside implication in receptor modulation and general cell physiology is rapidly accumulating: GM_1 may act as a receptor for extracellular signals, specifically Ca^{2+} ions, and take part in dynamic membrane functions (e.g., synaptic transmission) by undergoing phase transition in a lipid bilayer environment, by causing protein and/or lipid conformational changes within the bilayer via hydrogen bonding, and by acting as a water cavity (*54*) to modulate the local hydrophobicity of cell surface and events such as cell−cell and cell-protein interactions (*14*−*19*).

REFERENCES

1. Kanfer, J. N., and Hakomori, S. (1983) Sphingolipid Biochemistry. in *Handbook of Lipid Research* (Hanahan, D. J., Ed.) pp 89−165, 283−284, Plenum Press, New York.
2. Hill, M. W., and Lester, R. (1953) *Biochim. Biophys. Acta 282*, 18−30.
3. Ledeen, R. W., and Yu, R. K. (1982) *Methods Enzymol. 83*, 139−191.
4. Urban, P. F., Harth, S., Freysz, L., and Dreyfus, H. (1979) *Adv. Exp. Med. Biol. 125*, 149−157.
5. Felgner, P. L., Freire, E., Barenholz, Y., and Thompson, T. E. (1981) *Biochemistry 20*, 2168−2172.
6. Kalueff, A. V. (1996) *Ukr. Biokhim. Z. 68*, 15−19.
7. Nagai, Y. (1995) *Behav. Brain Res. 66*, 99−104.
8. Hakomori, S. (1996) *Adv. Pharmacol. 36*, 155−171.
9. Tsuji, S., Kojima, N., and Hitoshi, S. (1996) *J. Lipid Mediators Cell Signalling 14*, 289−294.
10. Pascher, I. (1976) *Biochim. Biophys. Acta 455*, 433−451.
11. Bertoli, E., Masserini, M., Sonnino, S., Ghidoni, R., Cestaro, B., and Tettamanti, G. (1981) *Biochim. Biophys. Acta 647*, 196−202.
12. Probst, W., Möbius, D., and Rahmann, H. (1984) *Cell. Mol. Neurobiol. 4*, 157−176.
13. Rahmann, H., Jonas, U., Kappel, T., and Hildebbrandt, H. (1998) *Ann. N.Y. Acad. Sci. 845*, 73−91.
14. Garcia, J. V., and Miller, A. D. (1991) *Nature 350*, 508−511.
15. Krifuks, O., Bergelson, L. D., and Schlesinger, M. (1998) *Cell. Immunol. 187*, 45−51.
16. Tiemeyer, M., Yasuda, Y., and Schnaar, R. L. (1990) *J. Biol. Chem. 264*, 1671−1681.
17. Higashi, H., Omori, A., and Yamagata, T. (1992) *J. Biol. Chem. 267*, 9831−9838.
18. Slenzka, K., Appel, R., and Rahmann, H. (1990) *Neurochem. Int. 17*, 609−614.
19. Hilbush, B. S., and Levine, S. M. (1992) *J. Biol. Chem. 267*, 24789−24795.
20. Dixon, S., Stewart, D., Grinstein, S., and Spiegel, S. (1987) *J. Cell Biol. 105*, 1153−1161.
21. Fishman, P. H. (1982) *J. Membr. Biol. 69*, 85−97.
22. Harris, P. L., and Thornton, E. R. (1978) *J. Am. Chem. Soc. 100*, 6738−6745.
23. Pascher, I., Lundmark, M., Nyholm, P. G., and Sundell, S. (1992) *Biochim. Biophys. Acta 1113*, 339−373.
24. Koerner, T. A. W., Prestegard, J. H., Demou, P. C., and Yu, R. K. (1983) *Biochemistry 22*, 2676−2687.
25. Abrahamsson, S., Dahlen, B., Lofgren, H., Pascher, J., and Sandell, S. (1977) Structure of Biological Membranes. in *The Structure of Biological Membranes* (Abrahamsson, S., and Pascher, J., Eds.) pp 1−23, Plenum Press, New York.
26. McDaniel, R. V., McLaughlin, A., Winiski, A. P., Eisenberg, M., and McLaughlin, S. (1984) *Biochemistry 23*, 1618−1624.
27. Wynn, C. G., and Robson, B. (1986) *J. Theor. Biol. 123*, 221−230.
28. Gammack, D. B. (1963) *Biochem. J. 88*, 373−383.
29. Folch, J., Lees, M., and Sloane-Stanley, G. H. (1957) *J. Biol. Chem. 226*, 497−509.
30. Svennerholm, L., and Fredman, P. (1980) *Biochim. Biophys. Acta 617*, 97−109.
31. Fredman, P., Nilsson O., Tayot, J. L., and Svennerholm, L. (1980) *Biochim. Biophys. Acta 618*, 42−52.
32. Iwamori, M., and Nagai, Y. (1978) *Biochim. Biophys. Acta 528*, 257−267.
33. Svennerholm, L. (1957) *Biochim. Biophys. Acta 24*, 604−611.
34. Kates, M. (1986) Technique of Lipidology: Isolation, Analysis and Identification of Lipids. in *Techniques in Biochemistry and Molecular Biology* (Burdon, R. H., and Knippenberg, P. H., Eds.) pp 100−278, Elsevier, New York.
35. Kauppinen, J. K., Moffatt, D. J., Mantsch, H. H., and Cameron, D. G. (1981) *Appl. Spectrosc. 35*, 271−276.
36. Cameron, D. G., and Moffatt, D. J. (1987) *Appl. Spectrosc. 41*, 539−544.
37. Kadowaki, H., Evans, J. E., and McCluer, R. H. (1984) *J. Lipid Res. 25*, 1132−1139.
38. Maggio, B., Albert, J., and Yu, R. K. (1988) *Biochim. Biophys. Acta 945*, 145−160.
39. Sonnino, S., Cantù, L., Corti, M., Acquotti, D., and Venerando, B. (1994) *Chem. Phys. Lipids 71*, 21−45.
40. Menikh, A., Nyholm, P. G., and Boggs, J. M. (1997) *Biochemistry 36*, 3438−3447.
41. Müller, E., and Blume, A. (1993) *Biochim. Biophys. Acta 1146*, 45−51.
42. Attar, M., Wong, P. T. T., Kates, M., Carrier, D., Jaklis, P., and Tanphaichitr, N. (1998) *Chem. Phys. Lipids 94*, 227−238.
43. Nabet, A., Boggs, J. M., and Pézolet, M. (1996) *Biochemistry 35*, 6674−6683.
44. Wong, P. T. T., and Mantsch, H. H. (1988) *Chem. Phys. Lipids 46*, 213−224.
45. Blume, A., Hübner, W., and Messner, G. (1988) *Biochemistry 27*, 8239−8249.
46. Hayashi, K., Mühleisen, M., Probst, W., and Rahmann, H. (1984) *Chem. Phys. Lipids 34*, 317−322.
47. Carrier, D., Chartrand, N., and Mattar, W. (1997) *Biochem. Pharmacol. 53*, 401−408.

48. Gurnani, K., Khouri, H., Couture, M., Bergeron, M. G., Beauchamp, D., and Carrier, D. (1995) *Biochim. Biophys. Acta 1237*, 86−94.
49. Sillerud, L. O., Schafer, D. E., Yu, R. K., and Königsberg, W. H. (1979) *J. Biol. Chem. 254*, 10876−10880.
50. Hinz, H. J., Körner, O., and Nicolau, C. (1981) *Biochim. Biophys. Acta 643*, 557−571.
51. Müller, E., Giehl, A., Schwarzmann, G., Sandhoff, C., and Blume, A. (1996) *Biophys. J. 71*, 1400−1421.
52. Hirai, M., and Takizawa, T. (1998) *Biophys. J. 74*, 3010−3014.
53. Baret, J. F., Bois, A. G., Dupin, J. J., and Firpo, J. L. (1982) *J. Colloid Interface Sci. 86*, 370−376.
54. Dahlen, B., and Pascher, I. (1979) *Chem. Phys. Lipids 24*, 119−133.
55. Boggs, J. M., and Koshy, K. M. (1994) *Biochim. Biophys. Acta 1189*, 233−241.
56. Maggio, B., Cumar, F. A., and Caputto, R. (1980) *Biochem. J. 189*, 435−440.
57. Jacques, L. W., Riesco, B. F., and Weltner, W. (1980) *Carbohydr. Res. 83*, 21−32.
58. Sharom, F. J., and Grant, C. W. M. (1978) *Biochim. Biophys. Acta 507*, 280−293.
59. Svennerholm, L. (1963) *J. Neurochem. 10*, 613−623.

BI9923104